# Effective pair potentials using an *ab initio* variational approach

Gérald Faussurier,[1,*] Christophe Blancard,[1] and Pier Luigi Silvestrelli[2,3]

[1]*CEA, DAM, DIF, F-91297 Arpajon, France*
[2]*Dipartimento di Fisica "G. Galilei," Università di Padova, via Marzolo 8, I-35131 Padova, Italy*
[3]*DEMOCRITOS National Simulation Center, 34014 Trieste, Italy*

We used a variational approach adapted to a quantum molecular-dynamics code to determine the best reference potential for warm dense aluminum. This *ab initio* variational approach was based on the Gibbs-Bogolyubov inequality. We used many-body reference systems interacting through inverse-power-law potentials, among which the Coulomb potential was a particular case defining the classical one-component plasma model. By comparisons with full quantum molecular-dynamics simulations, we found that the Coulomb potential was not always the best reference potential. We calculated the self-diffusion coefficient and the shear viscosity and discussed the results obtained using the Chisolm-Wallace relation in the warm dense matter regime.

PACS number(s): 71.15.Pd, 05.70.Ce, 71.15.Mb

## I. INTRODUCTION

Warm dense matter (WDM) is a fascinating field for which little is known both theoretically and experimentally.[1] WDM encompasses the first two decades of decreasing density below solid density up to density of the same order as a solid with temperatures from room temperature up to a few electron volts. In the WDM regime, matter is intermediate between the ordered solid and liquid phases and the highly disordered gas phase. This complex thermodynamic equilibrium regime makes the transition between solid-state physics to plasma physics. The WDM regime is typically encountered in planetary interiors, in cool dense stars, and in laboratory experiments.

WDM conditions are very difficult to create and properly characterize in laboratory. They open a challenging field of research for both experiments and *ab initio* calculations. At the present stage, measurements are scarce[2–15] and very few approaches can reproduce thermodynamic data and transport coefficients of such media in a self-consistent way.[16–20]

The most efficient and theoretical way to describe the WDM regime is the *ab initio* molecular-dynamics (AIMD) or quantum molecular-dynamics (QMD) approach.[21–26] This method incorporates at a high level of accuracy both ionic and electronic structure effects. It treats electron-ion and electron-electron interactions quantum mechanically in the framework of the density-functional theory and makes no *a priori* assumptions about ion-ion forces and the ionic structure. Though very powerful, the QMD method has intrinsic limitations. In fact, from one hand some approximations are involved, i.e., in the explicit form chosen for the exchange-correlation functional, in the calculation of the free energy, and in the pseudopotential approach. Indeed, the pseudopotential transferability could be only partial. From the other hand, the QMD method approach, due to its high computational cost, can be only applied to systems composed of a relatively small number of atoms and to relatively short MD simulations.

Recently, a method[27] has been proposed to face the problem of calculating the total free energy of the ionic and elec-tronic system with a QMD code using a reference system for the ionic subsystem and an *ab initio* variational approach based on the Gibbs-Bogolyubov inequality. Using the hard-sphere (HS) system as a reference system to describe the ionic structure, this *ab initio* variational approach has been shown to be more than ten times faster than QMD simulations. However, calculations were limited to the hard-sphere system, which may be too approximative to describe the ionic structure in the WDM regime.

In this paper, we applied the *ab initio* variational approach based on the Gibbs-Bogolyubov inequality using many-body systems interacting through inverse-power-law potentials as reference systems for the ionic structure. In Sec. II, we present the QMD code used and the *ab initio* variational approach based on the Gibbs-Bogolyubov inequality to calculate the total free energy of the ionic and electronic system. We detail how this variational method works for inverse-power-law potentials, including the Coulomb potential. Numerical results and comparisons to QMD simulations and measurements are performed and discussed in Sec. III for aluminum. We considered thermodynamic conditions encountered in x-ray Thomson scattering experiments.[28,29] By comparisons with full QMD simulations, we show that the classical one-component plasma, in a uniform background of opposite charge, is not always representative of the system under study. This illustrates the extreme difficulty to estimate *a priori* a reference system sufficiently close to the system under study in the WDM regime. Section IV is the conclusion.

## II. METHOD

### A. CPMD code

We used the CPMD code,[30,31] which has been improved by Alavi *et al.*[24] to study the electronic properties of metallic systems at finite temperature. This approach is based on the Mermin density-functional theory.[32] At each QMD step, a self-consistent electronic-structure calculation is performed, which takes into account the effect of thermal electronic ex-

citations consistently using fractionally occupied states. The interaction between ions and valence electrons is described using a pseudopotential. For a given configuration of $N_a$ ions $\{R_I\} \equiv \{R_1, \ldots, R_{N_a}\}$ inside a simulation box of volume $V_b$ with periodic boundary conditions, the electronic density $n(\mathbf{r})$ is computed by minimizing the free-energy functional $F_e$ of the electron gas. By construction, this functional $F_e$ reproduces the exact finite-temperature density of the Mermin functional. $F_e$, which is self-consistently optimized for each ionic configuration $\{R_I\}$, reads[33]

$$F_e = \Omega + \mu N_e + E_{II}, \tag{1}$$

where

$$\Omega = -\frac{2}{\beta}\ln \det[1 + e^{-\beta(\mathcal{H}-\mu)}] - \int d\mathbf{r}\, n(\mathbf{r})\left[\frac{\Phi(\mathbf{r})}{2} + \frac{\delta F_{xc}}{\delta n(\mathbf{r})}\right] + F_{xc}. \tag{2}$$

The factor two in front of the determinant logarithm stems from considering the spin-unpolarized special case only. $\beta = 1/k_B T$ with $T$ the electronic temperature and $k_B$ the Boltzmann constant, $\mu$ is the chemical potential, and $N_e$ is the total number of valence electrons. In Eq. (1) we have included the classical Coulomb energy of the ions $E_{II}$. The one-electron Hamiltonian

$$\mathcal{H} = -\frac{\nabla^2}{2} + V(\mathbf{r}) \tag{3}$$

is associated to the effective potential

$$V(\mathbf{r}) = \sum_I V_{eI}(\mathbf{r} - \mathbf{R}_I) + \Phi(\mathbf{r}) + \frac{\delta F_{xc}}{\delta n(\mathbf{r})}, \tag{4}$$

where $V_{eI}$ is the electron-ion potential, $\Phi$ is the Hartree potential of an electron gas of density $n(\mathbf{r})$, and $F_{xc}$ and the exchange-correlation free energy in the local-density approximation, respectively.[32,34–36] Thermodynamic equilibrium between electrons and ions is assumed in the simulations, so that the electronic temperature is equal to the average ionic temperature. The one-electron Hamiltonian is diagonalized by means of an efficient variant of the Lanczos algorithm. The electronic density is expressed in terms of single-particle orbitals $\Psi_k$

$$n(\mathbf{r}) = \sum_k \frac{|\Psi_k(\mathbf{r})|^2}{1 + e^{\beta(E_k - \mu)}}. \tag{5}$$

The chemical potential is adjusted such that $\int d\mathbf{r}\, n(\mathbf{r}) = N_e$. The electronic orbitals $\Psi_k$ are the one-electron eigenstates of $\mathcal{H}$ with eigenvalues $E_k$

$$\mathcal{H}\Psi_k(\mathbf{r}) = E_k \Psi_k(\mathbf{r}). \tag{6}$$

$\mathcal{H}$ is evaluated with $n(\mathbf{r})$ in this set of equations of the Kohn-Sham form. The ionic forces are calculated using the Hellmann-Feynman theorem.[37,38] The overall procedure ensures a self-consistent calculation of electronic and ionic structures. Once achieved the thermalization, one can select a set of uncorrelated QMD configurations on the fly as the simulation proceeds, and obtain that way, configuration-average quantities. Note also that the procedure of calculating configuration-average quantities by averaging over selected arrangements of atoms, and obtain that way results representative of the finite-temperature sample, induces an approximative treatment of the electron-phonon interaction. This "snapshot" treatment of the electron-phonon interaction makes sense at relatively high temperatures compared to the Debye temperature. This was the case in Refs. 19, 27, and 33 and for the thermodynamic situations encountered in the present work.

### B. *Ab initio* variational approach

A complete QDM simulations with the CPMD code can be quite time consuming. In practice, we often need to have a reasonably good representation of the interacting system of ions and electrons at finite temperature $T$ and mass density $\rho$ to test an assumption or to study the effect of one parameter. Recently, a powerful method has been proposed to determine the total free energy of the electron and ion system using the Gibbs-Bogolyubov inequality.[27] This approach works as follows. Assuming that we can describe atoms in disordered matter with a hard-sphere reference system, we dispatch $N_a$ nuclei inside a cubic supercell with periodic boundary conditions at given hard-sphere packing fraction $\eta$ using Monte Carlo simulations.[39] This is performed for a single element in thermodynamic equilibrium at given $\rho$ and $T$. For such an ionic configuration, we calculate the electronic free energy $F_e$ [Eq. (1)] with the CPMD code. We use a very good analytic expression for the excess ionic entropy per ion obtained by Carnahan and Starling.[40] We select $N_c$ statistically independent ionic configurations at given $\eta$. We then calculate the average $\langle F_e \rangle$ of $F_e$ over the $N_c$ configurations to obtain the reduced excess free energy $f_{exc}$ of the electron and ion system

$$f_{exc} = \beta \langle F_e \rangle / N_a + \frac{\eta(4 - 3\eta)}{(1-\eta)^2}. \tag{7}$$

It can be shown that $f_{exc}$ is an upper bound of the exact reduced excess free energy of the electron and ion system. The effective hard-sphere packing fraction $\eta_{eff}$ is found by minimizing $f_{exc}$ as a function of $\eta$ in Eq. (7). $\eta_{eff}$ is the optimum hard-sphere packing fraction in the sense of the Gibbs-Bogolyubov inequality. If we add to $f_{exc}$ in Eq. (7) the reduced free energy $f_0$ of the ideal gas,[41] we obtain the best total reduced free energy $f = f_0 + f_{exc}$ of the electron and ion system in the sense of the Gibbs-Bogolyubov inequality.[27] From $f$, we can derive in a self-consistent way the equation of state of the material. This method known as HS-AIMD for hard-sphere *ab initio* molecular dynamics[27] is faster that usual quantum molecular-dynamics simulations since no dynamics simulations are performed with the *ab initio* molecular-dynamics code. The HS-AIMD is a logical follow on to the work developed in the context of liquid metal[42,43] and later adapted and extended in the plasma physics field.[44,45] The HS-AIMD scheme has been compared successfully to quantum molecular-dynamics simulations and to experimental results.[27]

Using the hard-sphere system as a reference system may be too crude. Indeed, the variational method based on the Gibbs-Bogolyubov inequality to determine the total free energy of the electron and ion system works for any reference system described by many-body potential as long as the reduced excess configurational entropy of the reference system is known.[27] In this work, we propose to use the classical one-component plasma (OCP) in a uniform background of opposite charge and many-body systems interacting through inverse-power-law potentials.[46]

When the OCP is used, the particles of the reference system interact through the potential

$$\beta u(R) = \frac{\Gamma}{R},\tag{8}$$

where the distances are expressed in units of the ion-sphere radius or Wigner-Seitz radius $a_{WS}$. $a_{WS}$ is defined by the relation

$$\frac{4\pi}{3}\rho_i a_{WS}^3 = 1,\tag{9}$$

where $\rho_i = N_a/V_b$ is the particle density. In this particular case, a uniform background of charge is introduced to cancel the divergence due to distance images. Using convergence technique introduced by Ewald[47] and generalized by Nijboer and De Wette,[48] the particles of the reference system interact through the "Ewald potential" for which Hansen proposed a useful and accurate approximation based on Kubic harmonic expansion.[46] This approximation is fundamental for computer time requirement. The parameter $\Gamma$ introduced in Eq. (8) is a variational parameter. The optimum parameter $\Gamma_{eff}$ is determined by minimizing

$$f_{exc} = \beta\langle F_e\rangle/N_a - s_{exc}(\Gamma)\tag{10}$$

as a function of $\Gamma$. In Eq. (10), $s_{exc}(\Gamma)$ is the reduced excess configurational entropy of the OCP system. We used the most recent and accurate fit of the OCP equation of state proposed by De Witt and Slattery[49] to evaluate $s_{exc}(\Gamma)$. This fit was obtained from Monte Carlo simulations. As for the hard-sphere reference system, we dispatch $N_a$ nuclei inside a cubic supercell with periodic boundary conditions at given OCP parameter $\Gamma$ using Monte Carlo simulations to calculate $\langle F_e\rangle$ in Eq. (10). This method is called the OCP-AIMD approach.

When many-body systems interacting through inverse-power-law potentials are used as reference systems, the particles of the reference system interact through the potential

$$u(R) = \epsilon\left(\frac{\sigma}{R}\right)^n,\tag{11}$$

where $R$ is the interparticle distance. In fact, the configurational part of the thermodynamic quantities does not depend on temperature and density separately, but on their combination

$$z = (\rho_i\sigma^3)\left(\frac{\epsilon}{k_BT}\right)^{3/n}.\tag{12}$$

Thus, the properties computed along one isotherm or one isochore are sufficient to determine the thermodynamics in the whole density-temperature plane. Since we consider $n > 3$, we do not need to introduce any uniform background.[46,50] Inverse-power-law potentials defined by Eq. (11) are sometimes called soft-sphere potentials (SSP). The case $n = 12$ is important due to its obvious relation to the Lennard-Jones potential.[51] It is has been thoroughly investigated by computer simulations.[52,53] The cases $n = 4$, 6, and 9 have also been studied.[54] In this work, the parameter $z$ introduced in Eq. (12) is a natural variational parameter. The optimum parameter $z_{eff}$ is determined by minimizing

$$f_{exc} = \beta\langle F_e\rangle/N_a - s_{exc}(n,z)\tag{13}$$

as a function of $z$ at fixed $n$. In Eq. (13), $s_{exc}(n,z)$ is the reduced excess configurational entropy of the inverse-power-law system. We have used the variational modified hypernetted chain (VMHNC) (Ref. 55) theory to determine $s_{exc}(n,z)$ as a function of $n$ and $z$. The accuracy of the VMHNC theory is remarkable when compared to computer simulations.[56] In practice, we have calculated $s_{exc}(n,z)$ as a function of $z$ for various values of $n$ up to freezing and fit $s_{exc}(n,z)$ by a polynomial of order 5 (Ref. 57) in $z$. As in the previous cases, we dispatch $N_a$ nuclei inside a cubic supercell with periodic boundary conditions at given parameters $z$ and $n$ using Monte Carlo simulations to calculate $\langle F_e\rangle$ in Eq. (13). We called this method the SSP-AIMD approach. A similar method has been proposed by Greeff[58] using the reference potential $n = 12$ applied to the embedded atom model for copper.

### C. Free-energy calculation

The excess free energy determined by minimizing $f_{exc}$ in Eq. (7) and (10), or (13) is the best approximation to the exact excess free energy of the system in the sense of the Gibbs-Bogolyubov inequality. Indeed, there is an exact relation that gives the free energy $F$ of the system provided the free energy of the reference system $F_{ref}$ is known.[59,60] This relation reads

$$F = F_{ref} + \int_0^1 d\lambda\langle\Delta U\rangle_\lambda,\tag{14}$$

where $\Delta U$ is the difference between $F_e$ defined in Eq. (1) and the total energy of the reference system $U_{ref}$. Of course, both $F_e$ and $U_{ref}$ depend on the given configuration of $N_a$ ions $\{R_I\}$. $\langle\ \rangle_\lambda$ is the thermal average evaluated in the ensemble of the "intermediate" system whose total energy $U_\lambda = (1 - \lambda)U_{ref} + \lambda F_e = U_{ref} + \lambda\Delta U$. In practice, $\langle\Delta U\rangle_\lambda$ is evaluated at each value of the running coupling constant $\lambda$ using constant-temperature *ab initio* molecular dynamics generated by $U_\lambda$. If we combine this method with the variational approach, one uses a reference system which is the best in the sense on the Gibbs-Bogolyubov inequality, i.e., the closest to the real system whose dynamics is determined by $F_e$.

TABLE I. Effective ionic coupling parameter $\Gamma_{eff}$ and hard-sphere packing fraction $\eta_{eff}$ determined using the *ab initio* variational approach. We give the effective ionic coupling parameter $\Gamma_{TF}$ and the effective hard-sphere packing fraction $\eta_{TF}$ obtained using the Thomas-Fermi theory to calculate the average ionization and the screening length in the Yukawa approximation (Refs. 44 and 63–65) as well as the ionic coupling parameter $\Gamma_{val}$ obtained using a charge state equal to three. The last column refers to the sign of $\Delta f_{exc}$ $=f_{exc}^{OCP}-f_{exc}^{HS}$, where $f_{exc}^{OCP}$ and $f_{exc}^{HS}$ are the minimum excess free energy using OCP or HS reference system, respectively.

| $\rho$ (g/cm$^3$) | $T$ | $\Gamma_{val}$ | $\Gamma_{eff}$ | $\Gamma_{TF}$ | $\eta_{eff}$ | $\eta_{TF}$ | $\Delta f_{exc}$ |
|---|---|---|---|---|---|---|---|
| 2.0 | 1000 K | 860. | 81.1 | 47.0 | 0.37 | 0.34 | + |
| 2.0 | 5000 K | 172. | 25.3 | 11.3 | 0.26 | 0.19 | + |
| 1.7 | 5000 K | 163. | 20.2 | 9.1 | 0.22 | 0.17 | + |
| 1.4 | 5000 K | 153. | 12.1 | 7.0 | 0.18 | 0.14 | + |
| 1.4 | 8000 K | 95.5 | 10.4 | 4.8 | 0.16 | 0.11 | + |
| 1.4 | 10000 K | 76.4 | 9.5 | 4.0 | 0.15 | 0.10 | + |
| 3.4 | 1.1 eV | 80.4 | 30.9 | 9.9 | 0.29 | 0.18 | − |
| 3.7 | 5050 K | 209. | 92.5 | 25.3 | 0.40 | 0.28 | − |

## III. RESULTS AND DISCUSSION

### A. OCP

Calculations have been done with the CPMD code for aluminum using $N_a = 108$ and $N_c = 30$. The interaction between ions and valence electrons has been modeled using a norm-conserving pseudopotential with $s$ and $p$ nonlocalities.[61] The electronic orbitals were expanded in plane waves with a cut-off of 16 Ry. This aluminum pseudopotential has been carefully tested and successfully used in QMD simulations of solid and molten aluminum at the melting point[62] and to study metal-insulator transition in dense aluminum.[33] The $\Gamma$ point was used to sample the Brillouin zone of the supercell.[33] We present in Table I the results obtained with the *ab initio* variational approach using the OCP system as a reference system. We present the effective ionic coupling parameter $\Gamma_{eff}$ and hard-sphere packing fraction $\eta_{eff}$ determined using the *ab initio* variational approach. We considered thermodynamic conditions corresponding to the warm dense matter regime. Some cases were studied in Ref. 27 using the hard-sphere system as a reference system. We added cases relevant to recent x-ray Thomson scattering measurements.[28,29] Results are interesting and nontrivial. The effective ionic coupling parameter $\Gamma_{eff}$ is very different from the ionic coupling $\Gamma_{val}$ constant calculated using an ion charge state equal to three, i.e., the valence of aluminum. The fact that $\Gamma_{eff}$ differs from $\Gamma_{val}$ is due to screening and to the relaxation of electronic density while performing the minimization. From the effective hard-sphere packing fraction $\eta_{eff}$, one could use the mapping between the hard-sphere and the OCP systems based on the Gibbs-Bogolyubov inequality[44] to estimate an effective ionic coupling parameter. This method should be used with caution. The same remark applied to the Thomas-Fermi model used to calculate the average ionization and the screening length.[63–65] In this case, one considers a polarizable background and assumes a linear screening. This leads to a Yukawa (Y) potential.[29] Using the mapping between the hard-sphere and the OCP systems based on the Gibbs-Bogolyubov inequality[44] to esti-

mate an effective ionic coupling parameter $\Gamma_{TF}$ and an effective hard-sphere packing fraction $\eta_{TF}$ can give results in good agreement with the *ab initio* variational approach but this is not always the case. The discrepancy can also be noticeable. As expected, the effective parameters are increasing function of density at fixed temperature and decreasing function of temperature at fixed density. When we consider the sign of $\Delta f_{exc} = f_{exc}^{OCP} - f_{exc}^{HS}$, where $f_{exc}^{OCP}$ and $f_{exc}^{HS}$ are the minimum excess free energy using OCP or HS reference system, respectively, one can see that $f_{exc}^{OCP}$ is lower to $f_{exc}^{HS}$ only for the last two cases of Table I. This means that the OCP is better than the HS as a reference system, in the sense of the Gibbs-Bogolyubov inequality, only for these last two cases. On this example, the cases, for which the density is smaller than solid density ($\rho_S = 2.7$ g/cm$^3$), are better described by an HS reference system, whereas the cases, for which the density is larger than solid density are better described by an OCP reference system. Note that the agreement of the Thomas-Fermi predictions in the Yukawa approximation are the worst compared to the variational *ab initio* approach when the OCP system is the best reference system compared to the HS system. For the thermodynamic conditions encountered in this work, it has been found sufficient to determine $\eta_{eff}$ with an accuracy of 0.01. The minimum is well pronounced and a simple cubic fit of the excess free energy as a function of $\eta$ is enough to determine $\eta_{eff}$. The OCP system is more tricky since the minimum is very flat as a function of $\Gamma$ and the excess free energy is not always a symmetric function of $\Gamma$ close to the minimum. To determine $\Gamma_{eff}$, we changed $\Gamma$ to $\Gamma^s$, where $s = 0.323064$ is the power used to fit the part that is nonlinear in the excess internal energy of the OCP,[49] and we fit the excess free energy as a function of $\Gamma^s$ by a polynomial of order 5 to localize the minimum.

In Fig. 1, we consider aluminum at $\rho = 3.4$ g/cm$^3$ and $T = 1.1$ eV. We plot the pair-distribution functions obtained from QMD simulations,[29] the ones obtained from the OCP-AIMD method and the one deduced from the Y model and the VMHNC code (VMHNC-Y).[55,66] In Fig. 1, $\Gamma_{eff} = 30.9$ for
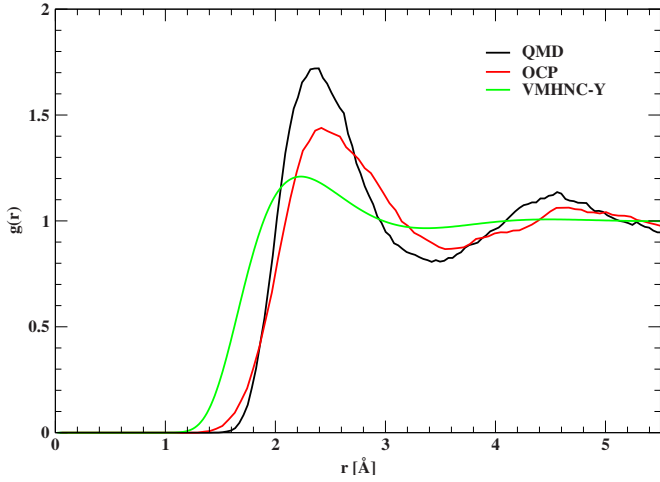
FIG. 1. (Color online) Pair-distribution function of aluminum at $\rho=3.4$ g/cm$^3$ and $T=1.1$ eV. Full QMD simulations (Ref. 29) are compared to the *ab initio* variational approach using an OCP system as a reference system and the VMHNC-Y approach.



FIG. 2. (Color online) Pair-distribution function of aluminum at $\rho=1.7$ g/cm$^3$ and $T=5000$ K. Full QMD simulations using the CPMD code (Ref. 33) are compared to the *ab initio* variational approach using an OCP system, a HS system, and a many-body system interacting through inverse-power-law potential ($n=13$) as reference systems.

the OCP case. The OCP result is in fair agreement with the QMD simulations. The VMHNC-Y result is in poor agreement with the QMD simulations. Indeed, the effective ionic coupling parameter that can be obtained from the Yukawa model[44,63–65] is equal to 9.9. This value departs noticeably from the value of 30.9 obtained using the *ab initio* variational approach. The Yukawa model does not describe properly screening due to electronic structure in the present condition. Similar results are obtained for aluminum at $\rho=3.7$ g/cm$^3$ and $T=5050$ K. Indeed, one can see that the QMD pair-distribution functions in these cases are smooth and trying to represent them by an OCP has meaning. But the agreement between QMD and OCP tends to deteriorate with decreasing density. As usual, the variational method based on the Gibbs-Bogolyubov inequality does its best to match QMD results. This means that the agreement is good when the reference system is sufficiently close to the real system. Note that results are good for the cases for which the OCP excess free energy is lower to the HS excess free energy. This indicates that the OCP is a better reference system than the HS reference system on these examples. This is what we can see by observing also the pair-distribution functions.

### B. Soft-sphere potentials

In Fig. 2 we consider aluminum at $\rho=1.7$ g/cm$^3$ and $T=5000$ K. We compare pair-distribution functions obtained with the *ab initio* variational approach to QMD simulations.[33] We can see that the HS potential ($\eta_{eff}=0.22$) is in good agreement between the decreasing part, just before the first minimum, and after the second maximum of $g(r)$. However, the first maximum is overestimated and the foot of the pair distribution is not well reproduced as expected. The OCP pair-distribution function ($\Gamma_{eff}=20.2$) really disagrees with the QMD simulations. The problem is not due to the *ab initio* variational approach. This discrepancy can be explained by the fact that at this thermodynamic condition, aluminum cannot be represented accurately by an OCP sys-
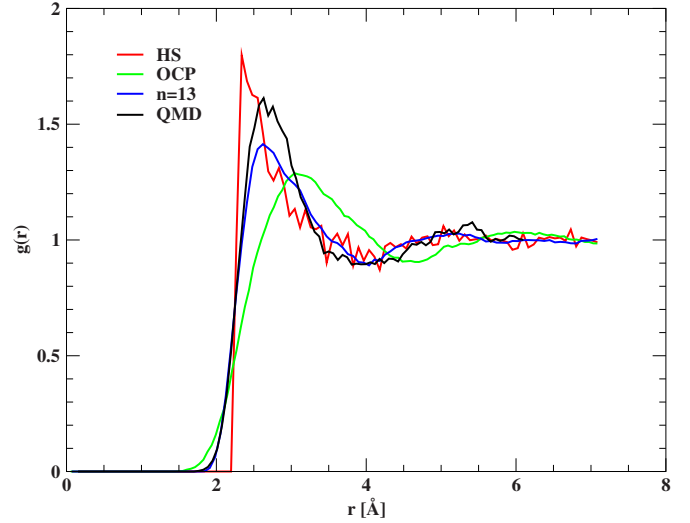
tem. The effective potential that could give the QMD pair-distribution function is more complicated than a simple Coulomb potential. In order to clarify this fact, we have used an inverse-power law potential to describe the reference system. We have considered $n=4-15$ considering every integer values between these two limits. We give in Table II the values of $z_{eff}$ obtained using the SSP-AIMD method for each value of $n$ corresponding to the cases presented in Table I when the HS reference system gives a lower excess free energy than the OCP reference system. The agreement between various values of $z_{eff}$ corresponding to different values of $n$ at given thermodynamic condition is due to roundoff. Like in the case of the hard-sphere system for $\eta_{eff}$, $z_{eff}$ was determined with an accuracy of 0.01. A fit of the excess free energy as a function of $z$ by a cubic polynomial was sufficient to determine $z_{eff}$. The HS reference system can be viewed as an inverse-power-law potential with $n=\infty$. The equivalent parameter $z_{eff}$ for the hard-sphere system is related to $\eta_{eff}$ by $z_{eff}=6\eta_{eff}/\pi$. The values of $\eta_{eff}$ shown in Table I are consistent with the values of $z_{eff}$ presented in Table II for large values of $n$. This consistency between the soft-sphere and the hard-sphere potentials is a stringent test for the method. This relation between hard-sphere and soft-sphere systems allowed ourselves to refine the determination of $\eta_{eff}$, especially at $\rho=1.7$ g/cm$^3$ and $T=5000$ K. The excess free energy as a function of $\eta$ was found to be very flat around the minimum in this case.[27] We have looked if the excess free energy is minimum for some value of $n$, i.e., $n_{min}$ at given density and temperature by including the hard-sphere cases. Results are given in Table II too. When temperature increases at constant density, the pair-distribution function $g(r)$ becomes broader. This means that the effective pair potential associated with $g(r)$ is softer. This explains why the case

TABLE II. Effective soft-sphere parameter $z_{eff}$ defined in Eq. (12) and determined using the *ab initio* variational approach. The integers are the powers introduced in Eq. (11). $n_{min}$ is the value for which the excess free energy is minimum at given density and temperature as a function of $n$.

| $\rho$ (g/cm$^3$) | $T$ (K) | $z_{eff}$ | | | | | | | | | | | | $n_{min}$ |
|---|---|---|---|---|---|---|---|---|---|---|---|---|---|---|
| | | 4 | 5 | 6 | 7 | 8 | 9 | 10 | 11 | 12 | 13 | 14 | 15 | |
| 2.0 | 1000 | 0.93 | 0.89 | 0.84 | 0.80 | 0.79 | 0.76 | 0.75 | 0.73 | 0.73 | 0.72 | 0.72 | 0.71 | >15 |
| 2.0 | 5000 | 0.68 | 0.65 | 0.60 | 0.55 | 0.54 | 0.53 | 0.53 | 0.51 | 0.51 | 0.51 | 0.51 | 0.50 | 14 |
| 1.7 | 5000 | 0.62 | 0.55 | 0.52 | 0.49 | 0.47 | 0.46 | 0.45 | 0.44 | 0.44 | 0.43 | 0.43 | 0.43 | 13 |
| 1.4 | 5000 | 0.50 | 0.47 | 0.43 | 0.40 | 0.38 | 0.38 | 0.36 | 0.35 | 0.35 | 0.35 | 0.35 | 0.35 | >15 |
| 1.4 | 8000 | 0.46 | 0.40 | 0.37 | 0.35 | 0.34 | 0.32 | 0.32 | 0.32 | 0.32 | 0.32 | 0.31 | 0.31 | 13 |
| 1.4 | 10000 | 0.42 | 0.38 | 0.34 | 0.33 | 0.31 | 0.31 | 0.30 | 0.30 | 0.30 | 0.29 | 0.29 | 0.29 | 13 |

$\rho=2.0$ g/cm$^3$ and $T=1000$ K has a strong HS-like character, which is strongly reduced when $\rho=2.0$ g/cm$^3$ and $T=5000$ K. Equivalent behaviors were found at $\rho=1.4$ g/cm$^3$ between 5000 and 10 000 K.

As an illustration, one can see in Fig. 2 that the QMD pair-distribution function obtained using an inverse-power-law potential with $n=13$ and $z_{eff}=0.43$ is well reproduced by the inverse-power-law potential as far as the foot and the raising part of $g(r)$ is concerned. Then, the first maximum is underestimated whereas the first minimum is overestimated by the inverse-power-law potential. The case $n=13$ with $z_{eff}=0.43$ is the best compromise to describe all the features of the QMD pair-distribution function. One can suggest that the effective potential that could reproduce the QMD pair-distribution function has an inverse-power-law component plus another component that is not easy to determine.

### C. Remarks

The cases discussed in this work span a very small part of the density-temperature plane for such a simple element as aluminum. However, we can see that the effective pair potential that can be representative enough of the system under study depends strongly on the thermodynamic situation. A great variety of behaviors is faced with whereas the thermodynamic domain considered is rather limited in temperature and density. This enlights the extreme difficulty to represent a system using an effective potential that can be representative enough of QMD simulations over an extended part of the density-temperature domain for multiscale applications. To do so, several steps are involved if, for instance, one is interested to obtain temperature and density-dependent effective potentials derived from QMD simulations. First, one has to choose a reference potential or a class of reference potentials representative of the material and of the thermodynamic conditions encountered. Second, one must know the reduced excess configurational entropy of the reference system that depends on the parameters defining the reference potential. For a pair potential, one can use the VMHNC approach to generate a data basis. For more complex potentials, one can use simulations, as was done for HS, OCP, Lennard-Jones, and SSP systems. Third, one has to find the best set of parameters in the sense of the Gibbs-Bogoluybov inequality

using a QMD code. The best potential is the one that gives the lowest minimum of the reduced excess free energy. One problem is related to the computation time needed to generate a data basis from (classical) simulations and to determine from (quantum) simulations the best potential that may depend on many parameters. Function minimization in a multidimensional space can be tricky. Another problem is to decide if the reference system is sufficiently close. It can be done during a simulation considering the minimum of the reduced excess free energy or by comparisons with QMD simulations for pair-distribution functions. However, some physical sense is required to select or eliminate from the start a set of potentials. Moreover, one cannot bypass close examination of results by comparisons with QMD simulations. Finally, one has to fit the parameters of the reference potential as function of density and temperature for multiscale applications and see what happens. The entire process relies on first principles that combines in a self-consistent way classical and quantum simulations. This strategy emphasizes the strong points of each approach and takes advantage of the computer resource available at the present time. Results presented in this paper can be understood as a demonstration of feasibility of extracting effective classical potentials from QMD simulations based on first principles. QMD codes are invaluable in this field. In summary, we hope to have shown that all the process has meaning and is worth applying in more specific and realistic cases.

### D. Effective ionization degree

The average ionization degree $Z^*$ is of fundamental interest when the system is ionized. However, it is difficult to determine it using a quantum molecular-dynamics code,[16,17] in an unambiguous way, in the WDM regime. We propose to determine $Z^*$ from the effective ionic coupling plasma parameter $\Gamma_{eff}$. We give in Table III the values of $Z^*$ corresponding to the thermodynamic conditions of Table I obtained from $\Gamma_{eff}$. We give also the values found using the Thomas-Fermi model.[63] We can see a large difference between the two ways to estimate $Z^*$. In particular, we should find $Z^* \sim 3$ at high density but we rather find $Z^* \sim 2$ from $\Gamma_{eff}$. This can be explained by the fact that $\Gamma_{eff}$ takes into account screening. Due to screening, $Z^*$ deduced from $\Gamma_{eff}$ is lower to the valence equal to three in all cases. This means

TABLE III. Effective ionization degree deduced from the Thomas-Fermi model (Ref. 63) and the effective ionic coupling parameter $\Gamma_{eff}$. In the latter case, expressing the ion-sphere radius $a_{WS}$ and $k_B T$ in atomic units, the effective ionization degree is equal to $\sqrt{\Gamma_{eff} a_{WS} k_B T}$, where $k_B$ is the Boltzmann constant and $T$ is the temperature.

| $\rho$ (g/cm$^3$) | $T$ | $Z^*_{OCP}$ | $Z^*_{TF}$ |
|---|---|---|---|
| 2.0 | 1000 K | 0.92 | 2.13 |
| 2.0 | 5000 K | 1.15 | 2.15 |
| 1.7 | 5000 K | 1.06 | 1.99 |
| 1.4 | 5000 K | 0.84 | 1.82 |
| 1.4 | 8000 K | 0.99 | 1.84 |
| 1.4 | 10000 K | 1.06 | 1.85 |
| 3.4 | 1.1 eV | 1.86 | 2.75 |
| 3.7 | 5050 K | 2.0 | 2.82 |

TABLE IV. Value of the dimensionless parameter $c = D \eta_s b / k_B T$ obtained using the hard-sphere ($c_{HS}$) or the OCP ($c_{OCP}$) reference systems. $k_B$ is the Boltzmann constant, $T$ is the temperature, $D$ is the self-diffusion coefficient, and $\eta_s$ is the shear viscosity. $b$ is a length on the order of the nearest neighbor and is related to the particle density $\rho_i$ by $b = 1/\rho_i^{1/3}$.

| $\rho$ (g/cm$^3$) | $T$ | $c_{OCP}$ | $c_{HS}$ |
|---|---|---|---|
| 2.0 | 1000 K | 0.12 | 0.16 |
| 2.0 | 5000 K | 0.08 | 0.16 |
| 1.7 | 5000 K | 0.09 | 0.17 |
| 1.4 | 5000 K | 0.12 | 0.21 |
| 1.4 | 8000 K | 0.13 | 0.23 |
| 1.4 | 10000 K | 0.15 | 0.25 |
| 3.4 | 1.1 eV | 0.08 | 0.16 |
| 3.7 | 5050 K | 0.13 | 0.17 |

that in the thermodynamic conditions presented in Table III, free electrons cannot be considered as a rigid neutralizing background with $Z^* \sim 3$ since they polarized around ions, $Z^*$ departing notably from the valence equal to three. The OCP is a highly idealized system that should be considered with caution when screening is important. The OCP-AIMD approach is a way to characterize the importance of screening by looking at the effective ionization degree extracted from the effective ionic coupling plasma parameter $\Gamma_{eff}$. The values presented in Table III are not easy to guess *a priori*, though the trend can be easily explained.

### E. Chisolm and Wallace relation

With the *ab initio* variational approach, we take into account the ionic structure explicitly. We have thus access to the ionic transport coefficients, such as the self-diffusion coefficient $D$ or the shear viscosity $\eta_s$. When the reference system is the HS system, we use the effective HS packing fraction $\eta_{eff}$ and the fits of the HS transport coefficients[44] derived from molecular-dynamics simulations.[41,67–71] When the reference system is the OCP, we use the effective ionic plasma coupling parameter $\Gamma_{eff}$ and the fits of the OCP transport coefficients[44] derived from molecular-dynamics simulations.[72,73]

The self-diffusion coefficient $D$ and the shear viscosity $\eta_s$ obey the Stokes-Einstein relation[41,74]

$$\frac{D \eta_s b}{k_B T} = c, \tag{15}$$

where $c$ is a dimensionless constant and $b$ is a length on the order of the nearest-neighbor distance. The compact Eq. (15) is a very efficient tool to have an indicator concerning the calculation of the self-diffusion coefficient and the shear viscosity. Taking $b = 1/\rho_i^{1/3}$ and using experimental values for $D$ and $\eta_s$, Chisolm and Wallace[74] found that $c = 0.18 \pm 0.02$ for 14 different liquid metals. In Table IV, we show the value of $c$ corresponding to the cases presented in Table I for the HS

($\eta_{eff}$) and the OCP ($\Gamma_{eff}$) reference systems. One can see that there is a clear discrepancy between HS and OCP predictions. Indeed, at melting ($\rho = 2.37$ g/cm$^3$ and $T = 933$ K), we found that $c = 0.18$ using the HS system, so in agreement with the value given by Chisolm and Wallace. However, we found $c \sim 0.15$ using the OCP system. The value obtained with the HS for dense cases are close 0.18. They depart from 0.18 for dilute cases only. This can be explained by the dependency of $c$ with respect to $\rho$ and $\eta_{eff}$, $c$ increasing with decreasing density. The HS system results do not appear to contradict the Chisolm and Wallace relation. This indicates that one tends to underestimate $c$ using the OCP system. Since the formulas used to estimate $D$ and $\eta_s$ are based on accurate molecular-dynamics simulations,[72,73] the OCP system is not well suited to describe the transport properties of WDM. The OCP system should be used with caution as a reference system both to describe the thermodynamic properties but also the transport properties of WDM.

### IV. CONCLUSION

Using a quantum molecular-dynamics code, we employed a variational approach based on the Gibbs-Bogolyubov inequality to determine the best reference potential for warm dense aluminum. We used many-body reference systems interacting through inverse-power-law potentials. By comparisons with full quantum molecular-dynamics simulations, we found that the Coulomb potential was not always the best reference potential. This work emphasizes the extreme difficulty to describe ions using analytical potential in the WDM regime.

*Corresponding author; gerald.faussurier@cea.fr

[1] R. W. Lee, H. A. Baldis, R. C. Cauble, O. L. Landen, J. S. Wark, A. Ng, S. J. Rose, C. Lewis, D. Riley, J.-C. Gauthier, and P. Audebert, Laser Part. Beams **20**, 527 (2002).

[2] A. W. DeSilva and J. D. Katsouros, Phys. Rev. E **57**, 5945 (1998).

[3] I. Krisch and H. J. Kunze, Phys. Rev. E **58**, 6557 (1998).

[4] J. F. Benage, W. R. Shanahan, and M. S. Murillo, Phys. Rev. Lett. **83**, 2953 (1999).

[5] J. F. Benage, Phys. Plasmas **7**, 2040 (2000).

[6] P. Renaudin, C. Blancard, G. Faussurier, and P. Noiret, Phys. Rev. Lett. **88**, 215001 (2002).

[7] P. Renaudin, C. Blancard, J. Clérouin, G. Faussurier, P. Noiret, and V. Recoules, Phys. Rev. Lett. **91**, 075002 (2003).

[8] V. N. Korobenko, A. D. Rakhel, A. I. Savvatimski, and V. E. Fortov, Phys. Rev. B **71**, 014208 (2005).

[9] J. Clérouin, P. Renaudin, Y. Laudernet, P. Noiret, and M. P. Desjarlais, Phys. Rev. B **71**, 064203 (2005).

[10] P. Renaudin, V. Recoules, P. Noiret, and J. Clérouin, Phys. Rev. E **73**, 056403 (2006).

[11] V. N. Korobenko and A. D. Rakhel, Phys. Rev. B **75**, 064208 (2007).

[12] J. Clérouin, V. Recoules, S. Mazevet, P. Noiret, and P. Renaudin, Phys. Rev. B **76**, 064204 (2007).

[13] J. Clérouin, P. Renaudin, and P. Noiret, Phys. Rev. E **77**, 026409 (2008).

[14] J. Clérouin, P. Noiret, V. N. Korobenko, and A. D. Rakhel, Phys. Rev. B **78**, 224203 (2008).

[15] A. W. DeSilva and G. B. Vunni, Phys. Rev. E **79**, 036403 (2009).

[16] M. P. Desjarlais, J. D. Kress, and L. A. Collins, Phys. Rev. E **66**, 025401(R) (2002).

[17] V. Recoules, P. Renaudin, J. Clérouin, P. Noiret, and G. Zérah, Phys. Rev. E **66**, 056412 (2002).

[18] S. Mazevet, M. P. Desjarlais, L. A. Collins, J. D. Kress, and N. H. Magee, Phys. Rev. E **71**, 016409 (2005).

[19] G. Faussurier, C. Blancard, P. Renaudin, and P. L. Silvestrelli, Phys. Rev. B **73**, 075106 (2006).

[20] N. Charpentier and J. Clérouin, Phys. Rev. B **78**, 100202(R) (2008).

[21] R. Car and M. Parrinello, Phys. Rev. Lett. **55**, 2471 (1985).

[22] M. C. Payne, J. D. Joannopoulos, D. C. Allan, M. P. Teter, and D. H. Vanderbilt, Phys. Rev. Lett. **56**, 2656 (1986).

[23] G. Kresse and J. Hafner, Phys. Rev. B **47**, 558 (1993).

[24] A. Alavi, J. Kohanoff, M. Parrinello, and D. Frenkel, Phys. Rev. Lett. **73**, 2599 (1994).

[25] P. Ordejón, E. Artacho, and J. M. Soler, Phys. Rev. B **53**, R10441 (1996).

[26] A. E. Mattsson, P. A. Schultz, M. P. Desjarlais, T. R. Mattsson, and K. Leung, Modell. Simul. Mater. Sci. Eng. **13**, R1 (2005).

[27] G. Faussurier, C. Blancard, and P. L. Silvestrelli, Phys. Rev. B **77**, 155126 (2008).

[28] E. García Saiz, G. Gregori, F. Y. Khattak, J. Kohanoff, S. Sahoo, G. Shabbir Naz, S. Bandyopadhyay, M. Notley, R. L. Weber, and D. Riley, Phys. Rev. Lett. **101**, 075003 (2008).

[29] K. Wünsch, J. Vorberger, and D. O. Gericke, Phys. Rev. E **79**, 010201(R) (2009).

[30] D. Marx and J. Hutter, *Modern Methods and Algorithms in Quantum Chemistry*, NIC Series Vol. 1 (NIC, Jülich, 2000), p. 301.

[31] The CPMD consortium at MPI für Festkörperforschung and IBM Research Laboratory, see also: http://www.cpmd.org

[32] N. D. Mermin, Phys. Rev. **137**, A1441 (1965).

[33] P. L. Silvestrelli, Phys. Rev. B **60**, 16382 (1999).

[34] P. Hohenberg and W. Kohn, Phys. Rev. **136**, B864 (1964).

[35] W. Kohn and L. J. Sham, Phys. Rev. **140**, A1133 (1965).

[36] W. Kohn and P. Vashishta, in *Theory of the Inhomogeneous Electron Gas*, edited by S. Lundqvist and N. H. March (Plenum, New York, 1983), p. 79.

[37] R. P. Feynman, *Statistical Mechanics* (Addison-Wesley, New York, 1972).

[38] J. Kohanoff, *Electronic Structure Calculations for Solids and Molecules: Theory and Computational Methods* (Cambridge University Press, Cambridge, 2006).

[39] W. Krauth, *Statistical Mechanics: Algorithms and Computations* (Oxford University Press, Oxford, 2006).

[40] N. F. Carnahan and K. E. Starling, J. Chem. Phys. **51**, 635 (1969).

[41] J.-P. Hansen and I. R. McDonald, *Theory of Simple Liquids*, 2nd ed. (Academic, London, 1986).

[42] N. W. Ashcroft and J. Lekner, Phys. Rev. **145**, 83 (1966).

[43] N. W. Ashcroft and D. Stroud, Solid State Phys. **33**, 1 (1978).

[44] G. Faussurier and M. S. Murillo, Phys. Rev. E **67**, 046404 (2003).

[45] C. Blancard and G. Faussurier, Phys. Rev. E **69**, 016409 (2004).

[46] J.-P. Hansen, Phys. Rev. A **8**, 3096 (1973).

[47] P. P. Ewald, Ann. Phys. (Leipzig) **369**, 253 (1921).

[48] B. R. A. Nijboer and F. W. De Wette, Physica (Amsterdam) **23**, 309 (1957).

[49] H. E. Dewitt and W. Slattery, Contrib. Plasma Phys. **39**, 97 (1999).

[50] J.-P. Hansen and D. Schiff, Mol. Phys. **25**, 1281 (1973).

[51] M. Ross, J. Chem. Phys. **71**, 1567 (1979).

[52] J.-P. Hansen, Phys. Rev. A **2**, 221 (1970).

[53] W. G. Hoover, M. Ross, K. W. Johnson, D. Henderson, J. A. Barker, and B. C. Brown, J. Chem. Phys. **52**, 4931 (1970).

[54] W. G. Hoover, S. G. Gray, and K. W. Johnson, J. Chem. Phys. **55**, 1128 (1971).

[55] Y. Rosenfeld, J. Stat. Phys. **42**, 437 (1986).

[56] B. B. Laird and A. D. J. Haymet, Mol. Phys. **75**, 71 (1992).

[57] D. A. Young and F. J. Rogers, J. Chem. Phys. **81**, 2789 (1984).

[58] C. W. Greeff, J. Chem. Phys. **128**, 184104 (2008).

[59] D. Alfè, G. D. Price, and M. J. Gillan, Phys. Rev. B **65**, 165118 (2002).

[60] M. J. Gillan, D. Alfè, J. Brodholt, L. Vocadlo, and G. D. Price, Rep. Prog. Phys. **69**, 2365 (2006).

[61] N. Troullier and J. L. Martins, Phys. Rev. B **43**, 1993 (1991).

[62] P. E. Blöchl and M. Parrinello, Phys. Rev. B **45**, 9413 (1992).

[63] R. M. More, Adv. At. Mol. Phys. **21**, 305 (1985).

[64] G. Chabrier, J. Phys. (France) **51**, 1607 (1990).

[65] A. Y. Potekhin, G. Chabrier, and D. Gilles, Phys. Rev. E **65**, 036412 (2002).

[66] G. Faussurier, Phys. Rev. E **69**, 066402 (2004).

[67] J. J. Erpenbeck and W. W. Wood, Phys. Rev. A **43**, 4254 (1991).

[68] B. J. Alder, D. M. Gass, and T. M. Wainwright, J. Chem. Phys. **53**, 3813 (1970).

[69] R. Grover, W. G. Hoover, and B. Moran, J. Chem. Phys. **83**, 1255 (1985).

[70] Y. Rosenfeld, J. Phys.: Condens. Matter **11**, 5415 (1999).

[71] S. Chapman and T. G. Cowling, *The Mathematical Theory of Non-Uniform Gases* (Cambridge University Press, New York, 1952).

[72] H. Ohta and S. Hamaguchi, Phys. Plasmas **7**, 4506 (2000).

[73] T. Saigo and S. Hamaguchi, Phys. Plasmas **9**, 1210 (2002).

[74] E. Chisolm and D. Wallace, *Shock Compression of Condensed Matter - 2005*, AIP Conf. Proc. No. 845 (AIP, New York, 2006), p. 53.